The control of cytochrome C oxidase on the cellular oxidative phosphorylation system depends on the mitochondrial energy state

Claudia Piccoli, Rosella Scrima, Domenico Boffoli, Nazzareno Capitanio

Biochemical Journal Immediate Publication. Published on 13 Mar 2006 as manuscript BJ20060077

THE CONTROL OF CYTOCHROME *C* OXIDASE ON THE CELLULAR OXIDATIVE PHOSPHORYLATION SYSTEM DEPENDS ON THE MITOCHONDRIAL ENERGY STATE.

Claudia Piccoli, Rosella Scrima, Domenico Boffoli, Nazzareno Capitanio[§]
Department of Biomedical Science, University of Foggia, Foggia, Italy, 71100.

Short (page heading) title: **metabolic flux control analysis of cytochrome c oxidase**

§ To whom correspondence should be addressed: Department of Biomedical Science, University of Foggia, viale L. Pinto OO.RR. 71100 Foggia, Italy. Tel.: +39 0881 711148; Fax +30 0881 714745; E-mail: n.cap@unifg.it

Recent measurements of the flux control exerted by cytochrome c oxidase on the respiratory activity in intact cells have led to a re-appraisal of its regulatory function. We have further extended this "*in vivo*" study in the framework of the metabolic control analysis and evaluated the impact of the mitochondrial transmembrane electrochemical potential ($\Delta\mu H^+$) on the control strength of the oxidase. The outcomes here presented show that, under conditions mimicking the mitochondrial state 4 of respiration both the flux control coefficient and threshold value of cytochrome oxidase are modified with respect to the uncoupled condition. The results obtained are consistent with a model based on changes in the assembly state of the oxidative phosphorylation enzyme complexes and the possible implication for the understanding of the exercise-intolerance of human neuro-muscular degenerative diseases is discussed.

INTRODUCTION

Mitochondrial oxidative phosphorylation (OXPHOS) constitutes the major cellular ATP producing mechanism under aerobic conditions. According to the chemiosmotic hypothesis the flux of electrons through the complexes of the respiratory chain from the (NADH and $FADH_2$)-linked substrates to O_2 is coupled to generation of a transmembrane protonmotive force ($\Delta\mu H^+$) across the inner mitochondrial membrane [1]. $\Delta\mu H^+$, constituted by an electrical and a chemical component ($\Delta\Psi$ and ΔpH respectively), is then exploited to drive endoergonic reactions like, first of all, the ATP synthesis by the F_o-F_1 H^+-ATP synthase. ATP generated in the mitochondrial matrix is then

exported to the cytoplasm by the adenine nucleotides translocator, in exchange with ADP, to fulfil the cytoplasmic energy demand. If the availability of ADP in the mitochondrial matrix becomes limiting, the transmembrane electro-chemical H^+ gradient accumulates and in turn inhibits further unnecessary electron transfer along the respiratory complexes. This negative loop allows modulating the rate of respiration to the cellular energy demand and constitutes the basis of the mitochondrial respiratory control [2].

The multi-components structuring of the OXPHOS network [3] poses the question to define which step(s) is(are) critical in controlling the efficiency of the overall process. The understanding of this specific point, besides its interest in basic research, is also important for elucidating the etiopathogenesis of a number of human diseases characterised by impairment in the OXPHOS efficiency [4]. The metabolic flux control analysis (MFCA) constitutes a solid theoretical and experimental tool that has contributed in our understanding of the molecular mechanism that determines how metabolic pathway fluxes are controlled [5,6]. It has been extensively applied to the mitochondrial OXPHOS system to estimate the control strength exerted by specific enzymatic steps to the overall process (i.e. respiratory rate and/or ATP synthesis) [7-9]. The survey of the results produced by these studies would indicate that the control of the OXPHOS system is shared among different steps with none of them showing a large control coefficient. As most of these studies have been carried out on isolated mitochondria and more recently on permeabilised cells [10,11], concern about the compliance of the conclusions to the "*in vivo*" situation has been raised [12-15]. Extension of the MFCA to intact cells has revealed, indeed, that cytochrome *c* oxidase (COX) exhibits a much lower reserve capacity than in isolated mitochondria thus promoting COX to a pivotal role in controlling respiration and OXPHOS.

It must be pointed out, however, that either "*ex vivo*" or "*in vivo*" MFCA of mitochondrial respiration, has been, almost exclusively, performed under uncoupled conditions (achieved in the presence of an excess of ADP or upon treatment of the sample with uncouplers of respiration) that limits the survey to a situation that does not encompass the physiological impact of the membrane potential on the mitochondrial OXPHOS performance. Therefore, the aim of this work was to explore if the depressing effect of the membrane potential on the overall mitochondrial respiration modifies the control strength exerted by a given isolated step (specifically COX) or simply superimposes a thermodynamic control without altering its kinetic reserve capacity.

Biochemical Journal Immediate Publication. Published on 13 Mar 2006 as manuscript BJ20060077

MATERIALS AND METHODS

Cell culturing.

The human hepatoma cell line HepG2 was maintained in culture with DMEM with 10% fetal bovine serum. Cells were allowed to grow to 70-80% confluence before harvesting. Cells were detached from 150 mm Petri dishes with 2 ml of trypsin-EDTA and washed in 20 ml phosphate buffer pH 7.4 (PBS) with 5% calf serum, centrifuged at 500xg, resuspended in 200 µl PBS, counted and immediately used. Cell viability as determined by trypan blue exclusion was typically never below 98%.

Mitochondria isolation, cytochrome c oxidase purification and liposome reconstitution. Mitochondria from bovine heart ("heavy" fraction) and rat liver were isolated by differential centrifugation as described in Ref.s 16 and 17respectively. Cytochrome *c* oxidase was purified from bovine heart mitochondria, as described in [18], tested for structural and functional parameters as in [19] and reconstituted in small unilamellar vesicles by the "cholate-dialysis" method [20]. The respiratory control ratio of cytochrome *c* oxidase vesicles was tested as in [20] and resulted routinely higher than 10.

Polarographic measurements.

The rate of oxygen consumption was measured polarographically with a Clark-type oxygen electrode in a thermostated chamber equipped with a magnetic stirring device (the instrumental setting was computer-controlled) and a gas-tight plugger endowed with a narrow port for additions by an Hamilton microsyringe. The medium/buffer used for measurement was 50 mM KH_2PO_4, 10 mM Hepes, 1 mM EDTA, pH 7.4, air-equilibrated at 37 °C (volume 0.5 ml) and the concentration of viable HepG2 cells was typically $10 \cdot 10^6$ cells/ml. Inhibition titration of the cellular respiratory activity was carried out by adding sequentially 0.5-1 µl of freshly prepared KCN solutions. The respiratory activities were corrected for the instrumental and/or medium-linked oxygen consumption drifts.

Laser scanning confocal microscopy analysis.

Cells were seeded at low density onto fibronectin coated 35 mm glass bottom dishes. After adhesion, living cells were directly incubated for 20 min at 37 °C with MitoCapture (1/1000 dilution, following the manufacturer recommendation). Then after cells were washed twice with PBS and examined by a Nikon TE 2000 microscope (images collected using a 60X objective (1.4 NA)) coupled to a Radiance 2100 dual laser (four-lines Argon-Krypton, single-line Helium-Neon) scanning confocal microscopy system (Biorad). The fluorescent signal of the double-emitter probe was examined sequentially, exciting first with the Ar-Kr laser beam (λ_{ex}=488 nm) and then with the

He-Ne laser beam (λ_{ex}=543 nm). Confocal planes of 0.2 µm in thickness were examined along the z-axes, going from the top to the bottom of the cells. Acquisition, storage and analysis of data were made by using LaserSharp and LaserPix software from Biorad. Quantification of the emitted fluorescent signal was achieved by producing a xz-intensity profile of the average value of the pixels within marked edges, including a single cell, as a function of each focal plane. Correction was made for minimal background by repeating the procedure in a cell-free field. The integrated value of the xz profile was taken as a measure of the fluorescence intensity of that individual cell.

Metabolic control analysis.

For the estimation of the control coefficient c_0 exerted by cytochrome c oxidase over the cell respiration two procedures were adopted. In one the ratios of the initial slopes from the cyanide titration curves of the integrated flow and isolated step were calculated by least square linear regression analysis. In this case the flux control coefficient is operatively defined as:

$$c_0 = (\Delta J_{IF}/\Delta[I])_{[I]=0}/(\Delta J_{IS}/\Delta[I])_{[I]=0}$$

where ΔJ_{IF} and ΔJ_{IS} are the changes of the respiratory rates of the integrated flow and isolated step respectively taken at the same interval of the inhibitor concentration, tending to 0.

The alternative procedure to calculate c_0 was that developed in [21] for non-competitive inhibition. In this case the final equation given in [21] was simplified as follow:

$$\% J/J_0 = 100 \cdot E / (c_0(E_0-E) + E)$$

with $E = -0.5(\alpha-\sqrt{(\alpha^2 + 4E_0K_D)})$

and $\alpha = [I] + K_D - E_0$

where: E and E_0 are the concentrations of the active enzyme at a given concentration of the inhibitor [I] and at [I]=0 respectively; K_D is the dissociation constant of the EI complex; J and J_0 are the respiratory rates measured at a given concentration of the inhibitor [I] and at [I]=0 respectively. With respect to the equation given in [21], an empirical exponent *n* was assumed to be 1 and as at high concentration of the inhibitor (*i.e.* E=0) the residual measurable respiratory rate was negligible, J_i was assumed to be 0 (cf. with eq. 5 in ref. 21). Imposing E_0=100, the entire data-set of the inhibitor titration curve for the integrated flow was fitted with the % of the un-inhibited activity given as a function of the concentration of the inhibitor. The parameters c_0 and K_D were estimated by the program GraFit 4.0.13 (Erithacus Software Limited). The accuracy of the fitting procedure was further tested by analysing the data of the inhibition titration curve for the isolated step. In this case c_0 was imposed to be 1 and the estimated K_D was verified to be comparable with that obtained from the fit of the integrated flow.

Kinetic simulation.

Modelling of a metabolic flow mimicking a multi-step electron transfer system was carried out with the freeware software package Chemical Kinetics Simulator (available at : http://www.almaden.ibm.com/st/ computational_science/ck/msim/). This program does not integrate sets of coupled differential equations to predict the time course of a chemical system. Instead, it uses a general, rigorously accurate stochastic algorithm to propagate a reaction. The stochastic method is comparable in efficiency to integration for simple kinetic schemes, and significantly faster for stiff systems [22].

Materials.

HepG2 cell line was from ATCC; DMEM, PBS, trypsin (0.05%)-EDTA(0.02%), penicillin (10000 U/ml)–streptomycin (10000µg/ml), fetal bovine serum from EuroClone; oligomycin, antimycin A, actractiloside, valinomycin, CCCP, cytochrome c from Sigma; ascorbate from Boehringer; TMPD from Fluka; Mitocapture from Biovision. All other chemicals were of the highest purity available.

Statistical analysis.

Two tailed Student's *t*-test was applied to evaluate the significance of differences measured throughout the data-sets reported.

RESULTS

Measurement of Endogenous Respiration and Cytochrome c Oxidase Activity in Intact Cells.

HepG2 is a human hepatoma cell line whose metabolism in the late exponential growth phase is mainly sustained by mitochondrial oxidative phosphorylation [23] and was therefore chosen for this study.

Fig. 1A shows a typical output of respirometric measurements for oxygen consumption, carried out on intact HepG2 cells. The respiratory rate was sustained by endogenous substrates and relied almost completely on the mitochondrial contribution as it was fully inhibited by KCN. The amount of the endogenous oxidiseble substrates was apparently never limiting since oxygen consumption was linear up to the instrumental detection limit (< 5% oxygen saturation). Addition of the ATP-synthase inhibitor oligomycin resulted in a marked depression of the oxygen consumption rate documenting the feature of an active phosphorylating state III for the endogenous respiration. The respiratory control ratio (state $III_{endogeneous}$/state $IV_{oligomycin}$) was 3.3 ±0.4 (n=10) (Fig. 1B). Atractiloside, an inhibitor of the mitochondrial adenine nucleotide translocator, resulted in depression of the endogenous respiration to an extent comparable with that attained by oligomycin

(data not shown). Uncouplers of the oxidative phosphorylation (DNP or CCCP) stimulated the oligomycin (or actractiloside)-settled respiratory rate but never exceeded that elicited in the state $III_{endogeneous}$ (data not shown).

These results confirmed qualitatively, at the cellular level, the bioenergetic paradigms well established in classical experiments carried out on isolated mitochondria [2] and showed that transmembrane potential exerts "*in vivo*" a tight control on respiration.

Fig.1A shows, also, that antimycin A, a specific inhibitor of cytochrome c reductase, completely inhibited endogenous respiration and that successive addition of ascorbate plus the membrane-permeant redox-recycling TMPD by-passed the block delivering electrons directly to cytochrome *c* oxidase *via* cytochrome *c* reduction. Unlike what was observed with the endogenous respiration, the ascorbate/TMPD-fuelled cytochrome *c* oxidase activity was only slightly blunted by oligomycin resulting in a respiratory control ratio of 1.3 $\pm$0.1 (n=6).

Measurement of Mitochondrial Membrane Potential in Intact Cells.

The involvement of the membrane potential in the control of mitochondrial respiration in intact cells was directly assessed by laser scanning confocal microscopy using the probe MitoCapture (Fig.2). Depending on the extent of the trans-membrane electrical potential the dye accumulates as monomer (green emitter) or dimer (red emitter, in iper-polirized mitochondria) resembling other dual emitters $\Delta\Psi$ probe [24]. Fig.2A shows that the fluorescence signal, due to accumulation of the probe in response to membrane potential was scantly detectable under condition of endogenous respiration but strongly increased (10 fold) when the cell samples were incubated with oligomycin. Coherently with the polarographic measurements Fig. 2 shows also that the membrane potential generated in the presence of oligomycin by COX was lower than that observed under endogenous respiration but however larger than that seen with the fully active ATP-synthase. This is not surprising as the proton-motive force generated by the cytochrome c oxidase is only a fraction of that produced by the entire respiratory chain which operates with the other two in-series proton pumping respiratory complexes (NADH dehydrogenase and cytochrome c reductase) [3]. Moreover it has been shown that the coupling efficiency of the COX redox-linked proton pump is negatively controlled by the extent of the Δp [25].

MCA of cytochrome c oxidase in intact cells.

The control exerted by COX over cell respiration and the effect on it of the mitochondrial membrane energization state was tested by applying the MFCA to intact cells. Fig. 3A shows the results of KCN titrations on the oxygen consumption rates sustained either by endogenous

substrates or by ascorbate plus TMPD. One can see that inhibition of the cell respiratory flux, resulted in a normalized titration curve almost super-imposable with that of the functionally isolated step. The flux control coefficient c_0 measured either by the ratio of the slopes attained in the initial low inhibitor concentration ranges and by non-linear fitting of the entire experimental data set of the integrated flow, was 0.6-0.7. When the same analysis was carried out with oligomycin pre-treated cells, the KCN-titration curve of the integrated flow revealed a much higher resistance to inhibition when compared with that of the isolated step and a more sigmoidal shape (Fig. 3B). The calculated c_0 was around 0.25.

The insert in Fig.3B shows that the KCN-inhibition titrations carried out on purified cytochrome oxidase reconstituted in liposomes under coupled (RCR ≥10) and uncoupled conditions resulted in super-imposable curves with practically identical Ki_{50} for KCN. This control clearly ruled out the possibility of an effect of $\Delta\Psi$ on the accessibility/affinity of CN- to the COX active site [26].

Fig. 3C shows that addition of KCN (up to 300 μM) to oligomycin-treated endogenously respiring HepG2 cells did not cause any appreciable change in the mt$\Delta\Psi$-dependent accumulation of MitoCapture. Some decrease of the fluorescent signal was recorded at 1 mM of the inhibitor. Thus, in spite of the inhibition of respiration the mt$\Delta\Psi$ was substantially maintained throughout the cyanide titration assay (see Discussion).

When the experimental data were graphed as a threshold plot, i.e. percentage of the endogenous respiratory activity as a function of the percentage of cytochrome c oxidase inhibition at the same KCN concentrations (Fig. 3D), a difference emerged. Whereas in the absence of membrane potential, COX exerted a strong control over the respiratory metabolic flux, such that any degree of inhibition of the isolated step resulted in an almost identical level of inhibition of the integrated respiratory flux, in the presence of oligomycin (i.e. with an established $\Delta\mu H^+$) the control strength of COX over the respiratory flux was reduced such that a 50-60 % inhibition of the isolated step resulted in only a 10 % decrease of the integrated flux. The threshold plots are usually characterized by a more evident biphasic behaviour with a net break point that allows for estimation of the threshold value [27]. Instead, the data presented here fit with a continuous curve which is however predicted by the metabolic control theory where it reveals the occurrence of compensatory changes of intermediates in the sequential array of enzymatic steps constituting the metabolic network [28] (see Discussion). In the presence of oligomycin a tentative threshold value might be set at around 75% inhibition of the isolated step. It must be mentioned, however, that a continuous curve in the threshold plot is not excluded. Further information deriving from the analysis of the threshold plot is the maximal reserve capacity of the isolated step that can be estimated by

extrapolation of the linear part of the threshold plot at the highest degrees of inhibition of the isolated step [13]. From the data shown in Fig. 3D it was estimated that the maximal reserve capacity of cytochrome c oxidase exceeded the theoretical capacity to sustain the full activity of the respiratory flux by 73% and 286% in the absence and in the presence of oligomycin respectively.

To exclude what observed was not due to undesired side-effect of oligomycin on cytochrome oxidase MFCA was carried out on HepG2 preincubated with oligomycin but in the presence of valinomycin plus CCCP. It can be seen that the fully uncoupling effect of the two ionophors resulted in a threshold curve that was undistinguishable from that obtained under endogenous respiration (Fig. 4 and cf. with Fig. 3D). Interestingly when the MCA was performed in the presence of oligomycin supplemented with sole valinomycin the threshold plot did not change with respect to that observed in the presence of oligomycin alone. As an enhancement of the DpH component of the $\Delta\mu H^+$ is expected to compensate for the K^+-valinomycin-mediated dissipation of the mt$\Delta\Psi$ [29], the result presented in Fig. 4 would suggest that the relative decrease of the COX-control strength on the cell respiration in the presence of a mitochondrial transmembrane protonmotive force is independent on which of the two thermodynamical components is operative with $\Delta\Psi$ and ΔpH being equally effective.

MCA of Cytochrome c Oxidase in Isolated Mitochondria.

The evidence here shown on one hand confirms what has been reported for other cell types in culture [12,13], and on the other hand contrasts with results of MFCA carried out on isolated mitochondria [7-9] which depending on the mammalian organ source resulted in a flux control coefficient for COX of 0.15-0.25 on the respiratory flux fuelled with either NADH-linked substrates or succinate [9]. Therefore we extended (as intra-lab control) the MFCA on mitochondria isolated from beef-heart and rat-liver. To rule out differences in the coupling efficiency that may arise from diverse protocols in the separation procedures we performed the MFCA on fully uncoupled frozen-thawed mitochondria. Fig. 5 illustrates the results obtained directly presented as threshold plot. It is shown that for the succinate-sustained respiratory flux COX displayed a very low reserve capacity (about 30%) and a c_0 of 0.7-0.8. As the freezing-thawing treatment of isolated mitochondria enables the substrate-binding site of complex I to be freely accessible it was also possible to apply the MFCA to respiratory flow directly fuelled by NADH. Also in this case, the threshold plot documented that for heart mitochondria a tight control of cytochrome oxidase with a maximal reserve capacity and control coefficient undistinguishable, on a statistical basis, from those measured for the succinate-sustained respiration. Addition of cytochrome c, to compensate for its possible loss from the mitochondrial intermembrane space, did not result in any significant

difference (data not shown). Surprisingly, when the same analysis was carried out on mitochondria isolated from rat liver the threshold curve for COX on the succinate-driven respiration was markedly different with a much lower control strength (both in terms of larger excess capacity and lower control coefficient). Table 1 summarizes the metabolic flux control parameters calculated for COX in all the conditions reported throughout this study.

DISCUSSION

The results here reported on the MCA of COX over the cell respiration resumed and extended previous studies carried out on intact cells. Under uncoupled conditions, it was confirmed that COX exhibits a low reserve capacity and a large control coefficient over the endogenous cell respiration but mimicking the state III of respiration by blocking the H^+ATP-synthase clearly showed that COX decreased its apparent control efficiency and that this effect can be attributable to the establishment of a steady-state $\Delta\mu H^+$. To our knowledge, this is the first case of a study carried out in intact cells, under close physiological conditions, where a comparison was made under two different bioenergetic states.

To avoid misinterpretations of the results we have carefully considered a number of points.

First, a criticism that could be raised to our experimental approach is that the membrane potential changed during the KCN inhibitory titration. We checked this specific point, and found that the addition of up to 300 μM cyanide (which caused 40% inhibition of the endogenous respiration in the presence of oligomycin) showed no effect on the "*in situ*" extent of mitochondrial $\Delta\Psi$. Some decrease of $\Delta\Psi$ was detected at 1 mM cyanide with a 70% inhibition of respiration. These results can be rationalised in terms of a non-ohmic flow-force relationship explainable in terms of a progressive change of either the passive proton conductance of the membrane [30] and/or the intrinsic the proton pumping efficiency of the respiratory chain complexes [31]. As the metabolic control coefficient c_0 was estimated from the ratio of the initial slopes of the integrated flow and the isolated step, it was, therefore, not affected by a decrease of the membrane potential that took place at much higher inhibition of the respiratory rates.

It might be argued that according to the summation principle a variation in the number of steps contributing to the metabolic flux would be expected to result in a re-distribution of the control coefficients whose sum must remain 1.0 [32]. Application of a static-head $\Delta\mu H^+$ on isolated mitochondria introduces, indeed, the H^+ back-leak as a new factor controlling the rate of respiration. Nevertheless the experiment on valinomycin-treated cells presented in Fig. 4 shows that substitution

of the trans-membrane electrical potential with a pH gradient resulted in no change of the COX control. Given the large difference in membrane conductivity of protons with respect to other cations or anions (the membrane conductance for H^+ is at least 10^6 times higher than for K^+ [33]) one would expect a tighter control of ΔpH in the metabolic network and as a consequence a compensatory decrease of the control coefficients of the other steps. But this was not the case for COX (cf. Fig. 3D and 4).

Another possibility that one could envision is that the membrane potential might change the catalytic features of cytochrome c oxidase (i.e. Km, Kcat) [34]. Given that the other complexes of the mitochondrial respiratory chain (which contain electrogenic steps in their catalytic mechanisms) would not escape the same possibility, differentiated variations in the relative catalytic features of the enzymatic steps in the network might cause a re-distribution of the control coefficients. Although this sounds plausible, it is not immediately clear how the conversion of an electrical potential in a pH gradient might mechanicistically produce the same effect. This would be the case if a protogenic step in COX (as well as in the other respiratory complexes) coincided with an electrogenic step that was rate-limiting, leaving this possibility very unlikely [35, 36].

The structural organization in the membrane of the many components of the mitochondrial OXPHOS system has been object in the past of a dispute with a model representing the enzymatic complexes acting as isolated entities in opposition to a model where the occurrence of a clustered structuring was considered [37, 38]. The latter hypothesis has been recently re-appraised on more solid experimental basis indicating the presence, in mitochondria of different species, of assembled super-complexes with defined stoicheiometry [38,39].

The so called “respirasomes” would gain a higher catalytic efficiency because of the channelling of mobile intermediates (like ubiquinol and cytochrome c) and of the contiguity between the $\Delta\mu H^+$ producers and utilizers. The alternative random collision controlled model, however, is not to be completely abandoned. Indeed one can envision a situation where the two organizational modes, respirasome *vs* isolated complexes, coexist in a dynamic equilibrium with the relative occupancy of the two structural subsets depending on the actual bioenergetic needs of the cell. The higher is the membrane potential the lower is, in principle, the energy demand of the cell because a slower rate of ATP utilization does not make available ADP for the ATP-synthase that in turn cannot dissipate the redox linked proton-motive force generated by the respiratory chain. Under this metabolic condition, the respirasome would dissociate in its constituting complexes and this would slow down the rate of oxygen consumption because diffusional steps between redox intermediates and enzymatic complexes are introduced. All the way around, when the cell hydrolyzes more ATP, because of a larger bioenergetic request, ADP is no longer a limitation for

the activity of the ATP-synthase, the transmembrane potential is promptly collapsed and the required higher rate of respiration satisfied by the assembly of the respiratory enzymes in super-complexes. Under this condition, the channelling of the redox intermediates will speed up the rate of electron transfer.

To test the hypothesis that a change in the control strength of an individual step might be featured in terms of equilibrium between different organizational structures of the enzymatic steps constituting the integrated flow, a mathematical simulation was performed. A simple electron transfer process was designed with three putative redox catalysts (X, Y, Z) transferring in sequence an electron from an initial donor (De^-) to a final acceptor (A). The three catalytic steps formed an assembled complex (XYZ) or alternatively were isolated from each other and the transfer of the electron was controlled by a channelled or collisional diffusion mechanism respectively (see schemes in Fig. 6). The results of a modelled inhibitory titration of the catalyst "Z" are shown in Fig. 6 as a threshold-like plot. One can see that when "Z" is part of the XYZ complex the overall rate of the flux correlates linearly with the amount of the controlling step, whereas when "Z" operates as an isolated step, a decrease in its amount, results in a clear deviation from a linear impact on the flux. It must be pointed out that in the two modelled conditions the rate constants for each simulated catalytic step were identical thus the change in the control exerted by the catalyst "Z" depends simply on the fact that when the catalyst is not complexed, its partial inhibition results in an increase of the steady-state concentration of Ye^- which reacting, accordingly to a second order reaction, with the residual fraction of the uninhibited "Z", compensates with a fractional increase of its actual transfer rate, the expected inhibition of the overall electron flux . This occurrence does not apply when "Z" is part of a complex because the intermediate $XYe^-Z_{inhibited}$ cannot transfer e- to the un-inhibited XYZ complexes. Consequently, that step will loose in controlling strength. In the framework of the metabolic control theory an identical result is predicted in the so called "network attenuation" [40] which however applies when each individual step of the network is working at a velocity substantially lower than their maximal velocity.

The above-depicted scenario implies that a change in the $\Delta\mu H^+$ itself might be at the same time the physiological signal and the trigger causing the structural re-organization of the enzymatic complexes of the mitochondrial OXPHOS system (see the model hypothesis in Fig. 7). Although the driving forces, leading to the assembly/disassembly of the super-complexes, have been not yet defined, it is not unconceivable that given the membrane-integrated nature of the single complexes, electrostatic as well as hydrophobic interactions must enter into play. Recent published observations have indicated for cardiolipin an essential role in promoting formation of mitochondrial respiratory supercomplexes [41]. Knocking-out the gene coding for the CL-synthase in yeast resulted, indeed,

in disappearance of the mitochondrial respirasomes, without affecting the catalytic activities of the isolated complexes [42]. Cardiolipin is a four acyl-tails anionic phospholipid with a large dipole potential, able to sense electrical gradient as well as pH (the pK_{a2} of the phosphate headgroup is ≥ 8, [43]) and to alter the physical properties of the membrane [44]. Moreover binding sites on the known crystallographic 3D structures of cytochrome c reductase and oxidase have been clearly localised [45,46]. Therefore cardiolipin (almost exclusively localised in the inner mitochondrial membranes) might well be the molecular sensor of the energy state of the mitochondrial membrane enabling the complexes of the OXPHOS system to change their assembly in response to the $\Delta\mu H^+$.

Consistent with our proposal are the results obtained with bovine heart isolated mitochondria confirming the tight control exerted by COX on the uncoupled NADH- or $FADH_2$-linked respiration. Cardiolipin, as well as the OXPHOS enzymatic-content, is known to vary in mitochondria from different organs with the heart being the richest one [47]. Mitochondria isolated from tissue relatively poorer in cardiolipin (like liver) or that are more vulnerable to modification during the isolation procedure (i.e. peroxidation) would tend to maintain the complexes isolated even in the absence of a membrane potential thus resulting in an apparent low flux control by COX.

The cardiolipin-mediated(controlled) change in the electrostatic/hydrophobic interaction of the mitochondrial OXPHOS complexes might provide therefore a “bioenergetic signal transduction” system that resembles the described function of plasma membrane rafts in stabilising a local platform for integrating the many components of the signal transduction network [48] though based on different membrane components.

Finally the observations reported here provide a rationale to understand some aspects of the stress-related symptoms of patients suffering of neuromuscular diseases caused by defects of the mitochondrial cytochrome c oxidase [49] or, more generally, by impairments of the OXPHOS system [4, 50]. Although the mitochondrial diseases encompass rare human inherited pathologies (1 case on 5000 newborns) the understanding of their ethiopatological mechanism may help in managing a larger number of more common pathologies where the involvement of defects in the mitochondrial respiratory chain has been defined [50]. The manifestation and severity of diseases linked to mutations in mtDNA is often correlated to its level of heteroplasmy [51]. In the same cell of a given tissue, mitochondria harbouring mutated and/or wild-type DNA can coexist. When the amount of mutated mtDNA is such that the gene product provided by the wild-type mtDNA does not compensate the defect of the mutated mtDNA, the bioenergetic competence of the cell is compromised. Thus a genetic threshold for the mutated mtDNA must be overcome to cause the disease to manifest and a wide array of clinical symptoms with different degree of severity may arise from the same mtDNA mutation depending on its level of heteroplasmy [28, 51]. A clinical

feature shared among patients suffering directly or indirectly of impairments of the COX complex is their intolerance to muscular work overload [52, 53]. An active state at the tissue-level (in terms of bioenergetic balance) means a condition of increased ATP consumption to perform work, which at the mitochondrial level produces a compensatory enhancement of the ATP-synthase activity given the larger availability of ADP and thus a decrease of the steady-state $\Delta\mu H^+$. Under this "stress" condition a defective COX activity will cause, according to our data, an almost proportional decrease of the overall aerobic flux which if not able to satisfy the enhanced bioenergetic demand will result in an unbalanced anaerobic cell metabolism. In addition to this, it is conceivable that an accumulation of redox intermediates up-hill of COX will favour formation of oxygen free radicals with further aggravation of the already debilitated patient conditions [54]. At rest, the same level of COX deficit might not be relevant because the re-distribution of the flux control coefficients will attenuate its impact on the overall respiratory rate.

ACKNOWLEDGEMENTS

The authors are grateful to Dr. Giuseppe Capitanio for having provided samples of beef heart and rat liver mitochondria and cytochrome oxidase vesicles. N.C. thanks Prof. Sergio Papa for continuous encouragement and critical reading of the manuscript and Dr. Gaetano Villani for stimulating discussion on the issues dealt within this paper. This work was supported by the University of Foggia Funds for Research "Quota progetti 2003-2004". The authors have no conflicting financial interests.

REFERENCES

1. Mitchell, P. (1966) Chemiosmotic coupling in oxidative and photosynthetic phosphorylation *Biol. Rev.* **41**, 445-502.
2. Chance, B. and Williams, C.R. (1955) Respiratory enzymes in oxidative phosphorylation. III. The steady state. *J. Biol. Chem.***217**, 409-427.
3. Saraste, M. (1999) Oxidative phosphorylation at the fin de siecle. *Science*. **283,** 1488-93.
4. Kang, D. and Hamasaki, N. (2005) Alterations of mitochondrial DNA in common diseases and disease states: aging, neurodegeneration, heart failure, diabetes, and cancer. *Curr Med Chem.***12**, 429-41.
5. Kacser, A. and Burns, J. A. (1973) In: Rate Control of Biological Processes (Davies, D.D. rd.), pp. 65-104, Cambrige University Press, London.
6. Heinrich, R. and Rapoport, T.A. (1974) A linear steady-state treatment of enzymatic chains. Critique of the crossover theorem and a general procedure to identify interaction sites with an effector. *Eur. J. Biochem.* **42**, 97-105.
7. Tager, J.M., Wanders, R.J., Groen, A.K., Kunz, W., Bohnensack, R., Kuster, U., Letko, G., Bohme, G., Duszynski, J. and Wojtczak, L. (1983) Control of mitochondrial respiration. *FEBS Lett.* **151**, 1-9.
8. Mazat, J.P., Letellier, T., Bedes, F., Malgat, M., Korzeniewski, B., Jouaville, L.S. and Morkuniene, R. (1997) Metabolic control analysis and threshold effect in oxidative phosphorylation: implications for mitochondrial pathologies. *Mol Cell Biochem*. **174,** 143-8.
9. Rossignol, R., Letellier, T., Malgat, M., Rocher, C. and Mazat, J.P. (2000) Tissue variation in the control of oxidative phosphorylation: implication for mitochondrial diseases. *Biochem J.* **347,** 45-53.
10. Saks, V.A., Veksler, V.I., Kuznetsov, A.V., Kay, L., Sikk, P., Tiivel, T., Tranqui, L., Olivares, J., Winkler, K., Wiedemann, F. and Kunz, W.S. (1998) Permeabilized cell and skinned fiber techniques in studies of mitochondrial function *in vivo*. *Mol. Cell. Biochem.*, **184**, 81–100.
11. Kunz, W.S., Kudin, A., Vielhaber, S., Elger, C.E., Attardi, G. and Villani, G. (2000) Flux control of cytochrome c oxidase in human skeletal muscle. *J Biol Chem.* **275,** 27741-5.
12. Villani, G. and Attardi, G. (1997) *In vivo* control of respiration by cytochrome *c* oxidase in wild-type and mitochondrial DNA mutation-carrying human cells. *Proc. Natl Acad. Sci. USA*, **94**, 1166–1171.

13. Villani, G., Greco, M., Papa, S. and Attardi, G. (1998) Low reserve of cytochrome c oxidase capacity in vivo in the respiratory chain of a variety of human cell types. *J Biol Chem.* **273,** 31829-36.
14. Villani, G. and Attardi, G. (2000) In vivo control of respiration by cytochrome c oxidase in human cells. *Free Radic Biol Med.* **29**, 202-10.
15. Villani, G. and Attardi, G. (2001)In vivo measurements of respiration control by cytochrome c oxidase and in situ analysis of oxidative phosphorylation. *Methods Cell Biol*. **65,** 119-31.
16. Low, H. and Vallin, I. (1963) Succinate-linked diphosphopyridine nucleotide reduction in submitochondrial particles. *Biochim. Biophys Acta* **69**, 301-302.
17. Bustamante, E., Soper, J.W. and Pedersen, P.L. (1977) A high-yield preparative method for isolation of rat liver mitochondria.*Anal Biochem.* **80**, 401-408.
18. Errede, B., Kamen, M.O. and Hatefi, Y. (1978) Preparation and properties of complex IV (ferrocytochrome c: oxygen oxidoreductase EC 1.9.3.1). *Methods Enzymol.* **53**, 40-47.
19. Capitanio, N., Vygodina, T.V., Capitanio, G., Konstantinov, A.A., Nicholls, P. and Papa, S. (1997) Redox-linked protolytic reactions in soluble cytochrome-c oxidase from beef-heart mitochondria: redox Bohr effects. *Biochim Biophys Acta* **1318**, 255-65.
20. Papa, S., Capitanio, N. and De Nitto, E. (1987) Characteristics of the redox-linked proton ejection in beef-heart cytochrome c oxidase reconstituted in liposomes. *Eur J Biochem*. **164**, 507-16.
21. Gellerich, F.N., Kunz, W.S. and Bohnensack, R. (1990) Estimation of flux control coefficients from inhibitor titrations by non-linear regression. *FEBS Lett*. **274**, 167-70.
22. Gillespie, D.T. (1976) A general method for numerically the stochastic time evoluyion of coupled chemical reactions. *Journal of Computational Physics* **22**, p 403.
23. Pinti, M., Troiano, L., Nasi, M., Ferraresi, R., Dobrucki, J. and Cossarizza, A. (2003) Hepatoma HepG2 cells as a model for in vitro studies on mitochondrial toxicity of antiviral drugs: which correlation with the patient? *J Biol Regul Homeost Agents.* **17,** 166-71.
24. Di Lisa, F., Blank, P.S., Colonna, R., Gambassi, G., Silverman, H.S., Stern, M.D. and Hansford, R.G. (1995) Mitochondrial membrane potential in single living adult rat cardiac myocytes exposed to anoxia or metabolic inhibition. *J Physiol*. **486,** 1-13.
25. Capitanio, N., Capitanio, G., Demarinis, D.A., De Nitto, E., Massari, S. and Papa, S. (1996) Factors affecting the H+/e- stoichiometry in mitochondrial cytochrome c oxidase: influence of the rate of electron flow and transmembrane delta pH. Biochemistry. *Biochemistry*. **35,** 10800-6.

26. Panda, M. and Robinson, N.C. (1995) Kinetics and mechanism for the binding of HCN to cytochrome c oxidase. *Biochemistry* **34,** 10009-18.
27. Rossignol, R., Malgat, M., Mazat, J.P. and Letellier, T. (1999)Threshold effect and tissue specificity. Implication for mitochondrial cytopathies. *J Biol Chem.* **274**, 33426-32.
28. Mazat, J.P., Rossignol, R., Malgat, M., Rocher, C., Faustin, B. and Letellier, T. (2001) What do mitochondrial diseases teach us about normal mitochondrial functions that we already knew: threshold expression of mitochondrial defects. *Biochim Biophys Acta*. **1504,** 20-30.
29. Cossarizza, A., Baccarani-Conti, M., Kalashnikova, G. and Franceschi, C. (1993) A new method for the cytofluorimetric analysis of mitochondrial membrane potential using the J-aggregate forming lipophilic cation 5,5',6,6'-tetrachloro-1,1',3,3'-tetraethylbenzimidazolcarbocyanine iodide (JC-1). *Biochem Biophys Res Commun*. **197**, 40-5.
30. Brand, M.D., Chien, L.F., Ainscow, E.K., Rolfe, D.F. and Porter, R.K. (1994) The causes and functions of mitochondrial proton leak. *Biochim Biophys Acta* **1187,** 132-9.
31. Zoratti, M., Favaron, M., Pietrobon, D. and Azione, G.F. (1986) Intrinsic uncoupling of mitochondrial proton pumps. 1. Non-ohmic conductance cannot account for the nonlinear dependence of static head respiration on delta microH.Biochemistry **25,** 760-7.
32. Brand, M.D., Vallis, B.P. and Kesseler, A. (1994) The sum of flux control coefficients in the electron-transport chain of mitochondria. Eur J Biochem. *Eur J Biochem.* **226,** 819-29.
33. Wrigglesworth, J.M., Cooper, C.E., Sharpe, M.A. and Nicholls, P. (1990) The proteoliposomal steady state. Effect of size, capacitance and membrane permeability on cytochrome-oxidase-induced ion gradients. *Biochem J*. **270,** 109-18.
34. Petersen, L.C., Degn, H. and Nicholls, P. (1977) Kinetics of the cytochrome c oxidase and reductase reactions in energized and de-energized mitochondria.*Can J Biochem*. **55**, 706-13.
35. Gregory, L. and Ferguson-Miller, S. (1989) Independent control of respiration in cytochrome c oxidase vesicles by pH and electrical gradients. *Biochemistry*. **28,** 2655-62.
36. Capitanio, N., De Nitto, E., Villani, G., Capitanio, G. and Papa, S. (1990) Protonmotive activity of cytochrome c oxidase: control of oxidoreduction of the heme centers by the protonmotive force in the reconstituted beef heart enzyme. *Biochemistry* **29,** 2939-45.
37. Hackenbrock, C.R., Chazotte, B. and Gupte, S.S. (1986) The random collision model and a critical assessment of diffusion and collision in mitochondrial electron transport. *J Bioenerg Biomembr*. **18,** 331-68.
38. Schagger, H. (2002) Respiratory chain supercomplexes of mitochondria and bacteria. *Biochim Biophys Acta.* **1555,** 154-9.

39. Bianchi, C., Genova, M.L., Parenti Castelli, G. and Lenaz, G. (2004) The mitochondrial respiratory chain is partially organized in a supercomplex assembly: kinetic evidence using flux control analysis. *J Biol Chem.* **279,** 36562-9.
40. Heijnen, J.J., van Gulik, W.M., Shimizu, H. and Stephanopoulos, G. (2004) Metabolic flux control analysis of branch points: an improved approach to obtain flux control coefficients from large perturbation data. *Metab Eng*. **4,** 391-400.
41. Pfeiffer, K., Gohil, V., Stuart, R.A., Hunte, C., Brandt, U., Greenberg, M.L. and Schagger, H. (2003) Cardiolipin stabilizes respiratory chain supercomplexes. *J Biol Chem*. **278**, 52873-80.
42. Zhang, M., Mileykovskaya, E. and Dowhan, W. (2005) Cardiolipin is essential for organization of complexes III and IV into a supercomplex in intact yeast mitochondria. *J Biol Chem.* **280,** 29403-8.
43. Haines, T.H. and Dencher, N.A. (2002) Cardiolipin: a proton trap for oxidative phosphorylation. *FEBS Lett*. **528**, 35-39.
44. Nichols-Smith, S. and Kuhl, T. (2005) Electrostatic interactions between model mitochondrial membranes. *Colloids Surf. B biointerfaces* **41**, 121-127.
45. Lange, C., Nett, J.H., Trumpower, B.L. and Hunte, C. (2001) Specific roles of protein-phospholipid interactions in the yeast cytochrome bc1 complex structure.*EMBO J*. **20,** 6591-600.
46. Mizushima, T., Yao, M., Inoue, N., Aoyama, H., Yamashita, E., Yamaguchi, H., Tsukihara, T., Nakashima, R., Shinzawa-Itoh, K., Yaono, R. and Yoshikawa, S. (1999) *Acta Crystallogr. Sect. A* 55, suppl., P06.04.069.
47. Agnati, L.F., Guidolin, D., Genedani, S., Ferre, S., Bigiani, A., Woods, A.S. and Fuxe, K. (2005) How proteins come together in the plasma membrane and function in macromolecular assemblies: focus on receptor mosaics. *J Mol Neurosci*. **26**, 133-54.
48. Fleischer, S., Rouser, G., Fleischer, B., Casu, A. and Kritchevsky, G.J. (1967) Lipid composition of mitochondria from bovine heart, liver, and kidney. *Lipid Res*. **8**, 170-80.
49. Pecina, P., Houstkova, H., Hansikova, H., Zeman, J. and Houstek, J. (2004) Genetic defects of cytochrome c oxidase assembly. *Physiol Res.* **53** Suppl 1:S213-23.
50. Wallace, D.C. (2005) A Mitochondrial Paradigm of Metabolic and Degenerative Diseases, Aging, and Cancer: A Dawn for Evolutionary Medicine. *Annu Rev Genet.* [Epub ahead of print]
51. Lightowlers, R.N., Chinnery, P.F., Turnbull, D.M. and Howell, N. (1997) Mammalian mitochondrial genetics: heredity, heteroplasmy and disease.*Trends Genet*. **13**, 450-5.

52. Taivassalo, T., Jensen, T.D., Kennaway, N., DiMauro, S., Vissing, J. and Haller, R.G. (2003) The spectrum of exercise tolerance in mitochondrial myopathies: a study of 40 patients. *Brain*. **126**, 413-23.
53. Elliot, D.L., Buist, N.R., Goldberg, L., Kennaway, N.G., Powell, B.R. and Kuehl, K.S. (1989) Metabolic myopathies: evaluation by graded exercise testing.*Medicine (Baltimore)* **68,** 163-72.
54. Papa, S. and Skulachev VP. (1997) Reactive oxygen species, mitochondria, apoptosis and aging.*Mol. Cell Biochem*. **174**, 305-319.

[1] *Abbreviations used*: OXPHOS, oxidative phosphorylation; MCA, metabolic control analysis; COX, cytochrome c oxidase; $\Delta\mu H^+$, electrochemical proton gradient; $\Delta\Psi$, transmembrane electrical potential; ΔpH, transmembrane pH gradient; DMEM, Dulbecco's modified Eagle medium; CCCP, carbonyl cyanide m-chlorophenyl-hydrazone; EDTA, ethylendiaminetetracetic acid; TMPD, N,N,N',N' tetramethyl-p-phenylenediamine.

Biochemical Journal Immediate Publication. Published on 13 Mar 2006 as manuscript BJ20060077

Table 1 MFCA of cytochrome c oxidase on the respiratory activity of intact cells and isolated mitochondria.

Summary of the results presented throughout the paper. c_0: control coefficient calculated from the CN titration curves either by dividing the slopes attained in the initial low inhibitor concentration ranges and by non-linear fitting of the entire experimental data set of the integrated flow (see under Materials and Methods); the values reported are the averages of the results obtained by the two procedures differing by less than 10%. MRC: maximal reserve capacity, calculated from the threshold plots by extrapolating to 0% COX activity the experimental points attained at the highest inhibitor concentration. Thresholds values refer to the intercepts of the straight lines of the experimental points attained at the lowest and highest inhibitor concentrations and interpolated on the % COX inhibition axe. For experimental details see legends to Figures 3-5.

Sample	Respiratory substrate(s) /conditions	Cytochrome c Oxidase		
		c_0	MRC	Threshold
Intact HepG2 cells	End. resp.	0.68 ±0.04	173	48.5
Intact HepG2 cells	End. resp. + olig.	0.25 ±0.03	386	74.5
Intact HepG2 cells	End. resp. + olig., val.	0.22 ±0.07	315	77.9
Intact HepG2 cells	End. resp. + olig., val., CCCP	0.63 ±0.02	140	52.9
Beef-heart mitochondria	Succinate	0.90 ±0.03	107	48.3
Beef-heart mitochondria	NADH	0.85 ±0.04	110	49.4
Rat-liver mitochondria	Succinate	0.15 ±0.05	314	73.2

Biochemical Journal Immediate Publication. Published on 13 Mar 2006 as manuscript BJ20060077

FIGURE LEGENDS

Figure 1. Measurement of O_2 consumption rates in HepG2. A: polarographic traces showing the endogenous respiration in intact cells (on the left) and the *in situ* activity of cytochrome c oxidase (on the right). In the latter case the endogenous respiration was inhibited by 1 μg/ml antimycin A and the cytochrome oxidase activity was rescued by addition 10 mM ascorbate plus 200 μM of the membrane permeant TMPD. Where indicated 2 μg/ml oligomycin and 2 mM KCN were added. The changes in the rates of O_2 consumption, throughout the assays, are given as first derivative in the panels below the corresponding traces. B: statistical evaluation of the effect of oligomycin on the activities of the respiratory endogenous flow (±S.E.M., n=10) and cytochrome c oxidase isolated step (±S.E.M., n=6). The respiratory control ratios of the rates of O_2 consumption in the absence and in the presence of oligomycin is also shown. Paired Student's *t* test analysis: *, $P<0.05$; **, $P<0.001$.

Figure 2. **Confocal microscopy analysis of respiration-driven mitochondrial membrane potential in HepG2.** A: imaging of the fluorescence signal of the probe MitoCapture in live cells. The upper two panels show the analysis carried out under respiratory conditions sustained by endogenous substrates (on the left) and by activation of cytochrome c oxidase as isolated step (on the right). The lower two panels show the effect of pre-incubation of the cells with 2 μg/ml oligomycin on the mitochondrial membrane potential generation under endogenous (on the left) and isolated step (on the right) respiratory activities. The images shown are superimposition of confocal planes and are representative of 4 different experiments. B: single cells analysis of the green fluorescence intensity of MitoCapture under the four conditions described in A. The fluorescence intensities were quantified as described in Materials and Methods and normalised to the surface of the selected area; 20-30 cells were analysed for each condition and the results shown are averages (±S.E.M.) of the experiment shown in A. Results of paired Student's *t* test analysis for the fluorescence intensity of oligomycin-untreated vs oligomycin-treated cells: *, $P<0.01$; **, $P<0.001$.

Figure 3. Metabolic control analysis of cytochrome c oxidase over the endogenous respiration in intact HepG2 cell line: effect of $\Delta\mu H^+$. Titration curves for KCN inhibition of the endogenous respiration (black circles) and of ascorbate/TMPD-dependent respiration (white circles) in the absence (**A**) and in the presence (**B**) of oligomycin. The residual activity is given as percentage of the un-inhibited respiratory rate. See legend to Fig. 1A and Materials and Methods for experimental details. The data points shown are the averages of at least 5 different titrations (± S.E.M.) for each condition. P represents the statistical significance provided by the Student's *t* test analysis when

applied to the data points for the endogenous and COX activity in the [KCN] range from 50 to 500 μM. The solid lines are the best fit of the data points obtained applying the equation for non-linear regression analysis given in Materials and Methods; parameters setting: K_D=130±7 μM and 90±7 μM for the endogenous fluxes without and with oligomycin respectively, with the relative computed c_0 values indicated in the panels. When the control coefficients were calculated from the ratios of the initial tangents of the integrated vs the isolated steps values of 0.65 and 0.22 were estimated. The inset in panel B shows KCN titration curves for purified beef heart cytochrome c oxidase reconstituted in liposomes; the concentration of cytochrome oxidase vesicles was 50 nM and the respiratory activity was measured polarographically (as in Fig. 1A) in the presence of 10 mM ascorbate, 200 μM TMPD and 20 μM cytochrome c under coupled (white squares) and fully uncoupled (valinomycin + CCCP) (black squares) conditions (average of two experiments). C: Confocal microscopy analysis by MitoCapture of the effect of KCN titration on the mitochondrial membrane potential in cells respiring with endogenous substrates in the presence of oligomycin. The experimental conditions are those illustrated for panel B. KCN was added, at the indicated concentrations, directly to the dishes 5 min before the addition of Mitocapture. For comparison, imaging of the ΔΨ-probe in HepG2 respiring in the absence of oligomycin is shown under identical instrumental setting conditions. The bars quantify the relative fluorescence (RF) signal (green emission) in the oligomycin-treated cells normalised to that of the cells respiring in the absence of oligomycin (see legend to Fig. 2B for the quantification procedure). The images selected are superimposition of confocal planes and are representative of three independent experiments. See Materials and Methods for further details. D: threshold plots for COX activity over the endogenous respiration in the absence (white squares) and in the presence (black squares) of oligomycin are from the inhibitor titration data presented in panels A and B respectively. The solid lines derive from the combination of the equations fitting the titration curves in A and B. The arrows indicate the threshold values for the two plots obtained from the intercepts of the lines tangent to the initial and final part of the curves. The calculated values for the threshold points are around 40 % and 75 % of COX inhibition for the plots obtained in the absence and in the presence of oligomycin respectively. The insert in C shows an expantion of the same plot along the ordinate axis enabling to pinpoint the maximum COX capacities as intercepts from the extrapolated lines fitting the points at the highest % of COX inhibition [12,13].

Figure 4. Effect of ionophores on the threshold plots for COX activity over the endogenous respiration in oligomycin-treated HepG2 cells. The experimental conditions for the inhibitor titrations are similar to those shown in Fig.1-panel B but cells were pre-incubated with 4 μg/ml

valinomycin alone (black squares) o in combination with 4 μM CCCP (white squares). The data points are the average of three independent experiments for each condition (± S.E.M.). The panels on the right are the imaging by confocal microscopy analysis illustrating the effect of valinomycin without and with CCCP on the mitochondrial $\Delta\Psi$ in cells respiring with endogenous substrates in the presence of oligomycin. Ionophores were added directly to the dishes 5 min before the addition of the probe Mitocapture, at the concentrations used for the KCN titration assays. For comparison, the imaging of cells untreated with ionophores is also shown.

Figure 5. Metabolic control analysis of cytochrome c oxidase in isolated mitochondria. 1 mg prot/ml of frozen-thawed mitochondria isolated from beef heart (BHM, closed symbols) or rat liver (RLM, open symbols) were fuelled with 200 μM NADH (squares) or 5 mM succinate (circles) (in the presence of 1μg/ml rotenone) and the respiratory rates subjected to KCN inhibition titration. Identical KCN range was used to titrate the activity of cytochrome c oxidase as isolated step sustained by 10 mM ascorbate plus 0.2 mM TMPD. The results of the inhibition titrations are directly shown as threshold plots of the COX activity on the NADH- and succinate-sustained respiration.

Figure 6. Kinetic simulation of the metabolic flow throughout aggregated or isolated steps: effect on the control of a single step. A metabolic flow mimicking electron transfer throughout three enzymatic steps from an initial donor De- to a final acceptor A was simulated. Two models were tested: in one the three steps were assumed to be physically assembled in a single complex with an internal e- transfer (model A), in the other the three steps were assumed to be isolated and the e- transfer occurred by stochastic events controlled by random collision. In addition one of the three putative enzyme (Z) was possibly blocked by an inhibitor I. The rates of the overall simulated e- transfer to the acceptor was estimated in the presence of increasing concentrations of the inhibitor inducing a progressive 10% stepwise inhibition of the isolated step irrespective of its assembly state. The graph reports as threshold plots the results of the simulations for both models. The numerical values for the kinetic constants where: 1.0 for steps 1- 4, 8 and 100 for steps 5-7, in simulation (A) and 1.0 for steps 1-4 and 100 for step 5, in simulation (B). See under Materials and Methods for details on the software used.

Figure 7. Schematic working model illustrating the effect of the mitochondrial membrane energy state on the super-molecular structure of the enzymatic components of the OXPHOS system. The respiratory complexes are illustrated as boxes embedded in the inner mitochondrial

membrane (IMM). The stoicheiometry of the complexes in the “respirasomes” shown in the upper part of the scheme are purely indicative [see ref. 38 for experimentally defined stoicheiometries]. Moreover the assembled supercomplexes might include the H+-ATP-synthase and mitochondrial substrate carriers as well. The graphs on the right show the expected threshold plots of the major controlling isolated step on the basis of a combination of kinetic and thermodynamic features in the two assembly-states (see Discussion).

Biochemical Journal Immediate Publication. Published on 13 Mar 2006 as manuscript BJ20060077

Fig. 1

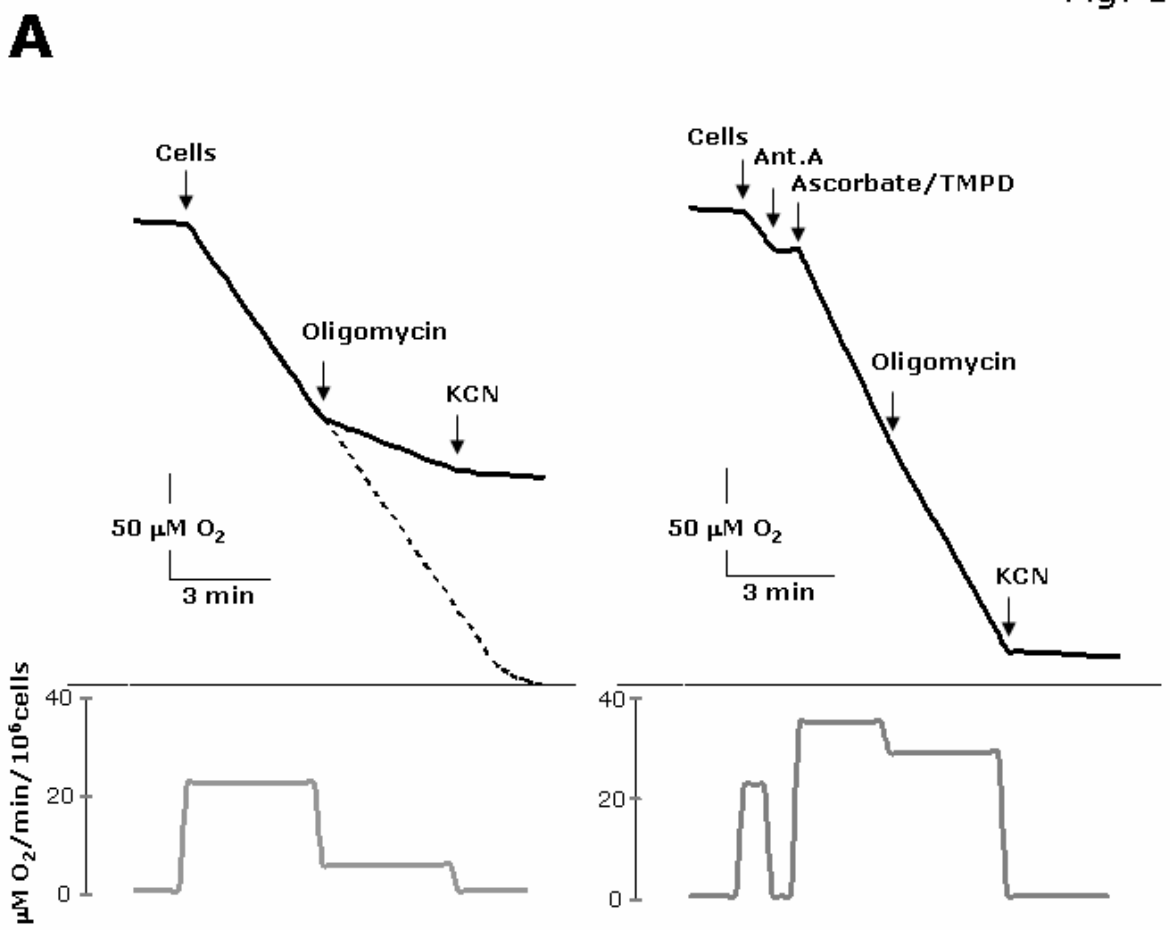

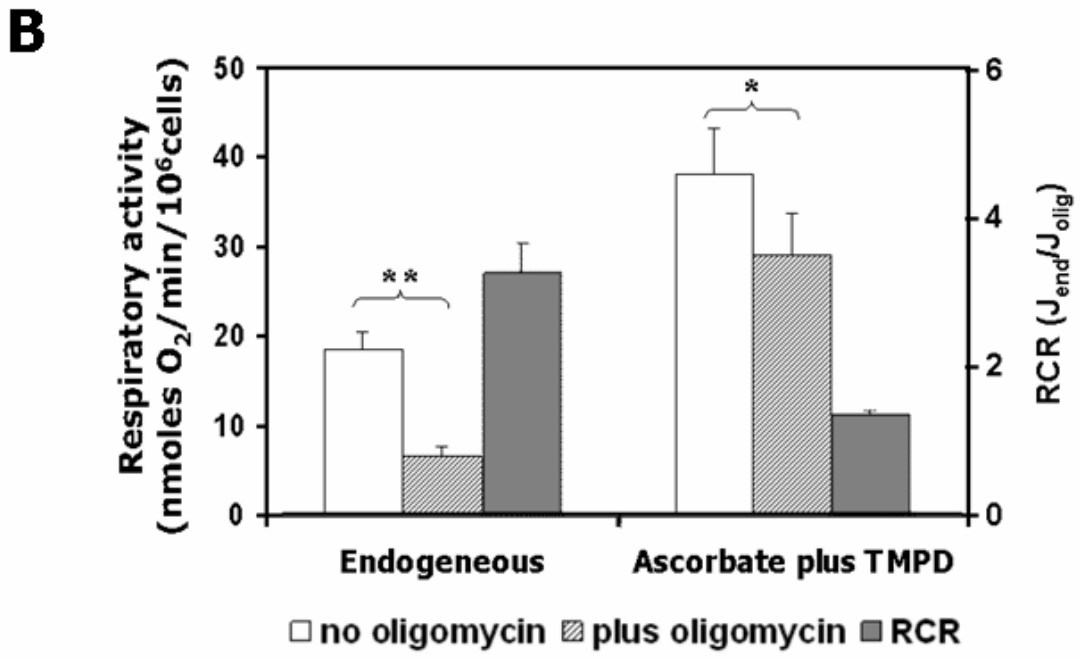

Biochemical Journal Immediate Publication. Published on 13 Mar 2006 as manuscript BJ20060077

Fig. 2

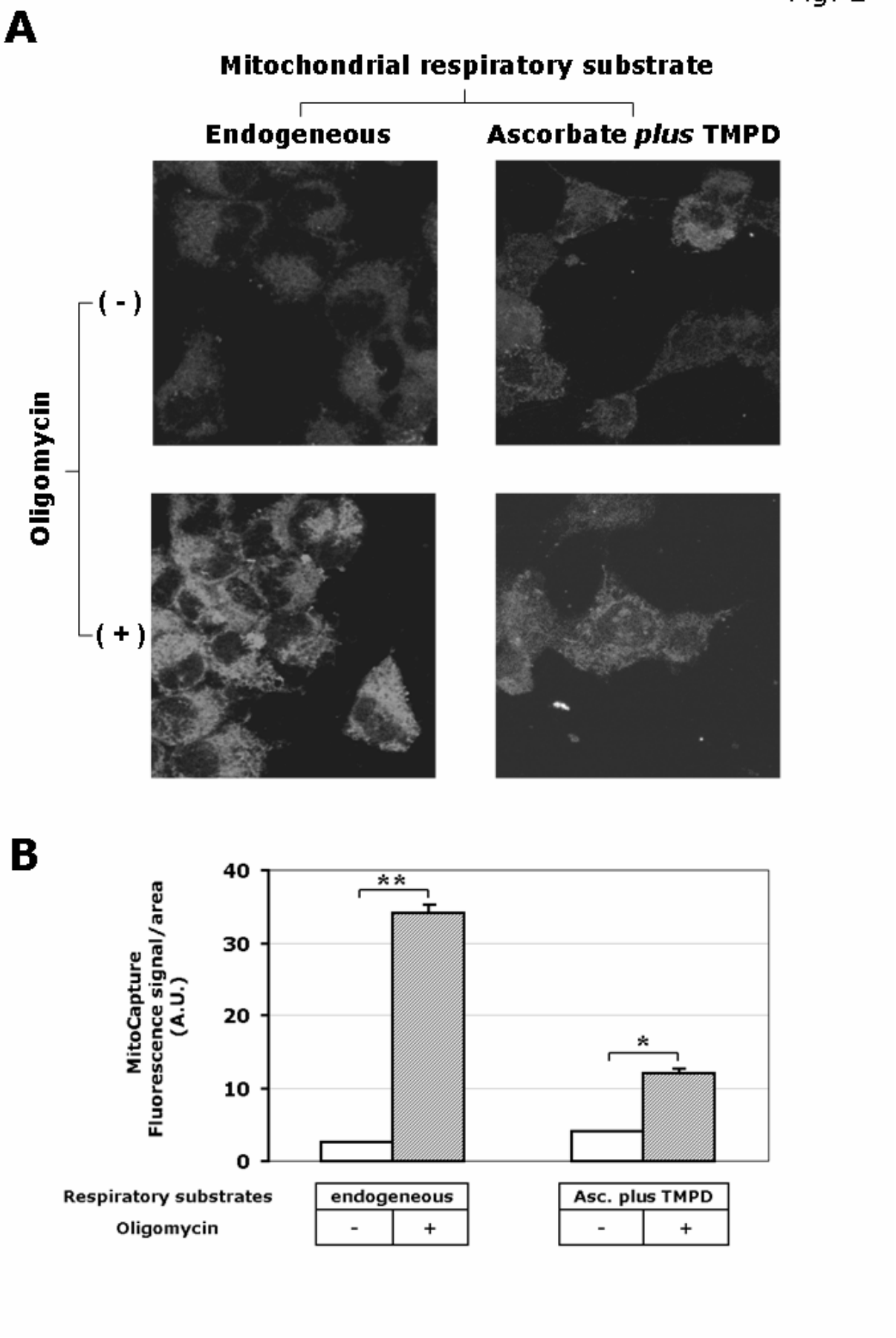

Biochemical Journal Immediate Publication. Published on 13 Mar 2006 as manuscript BJ20060077

Fig. 3

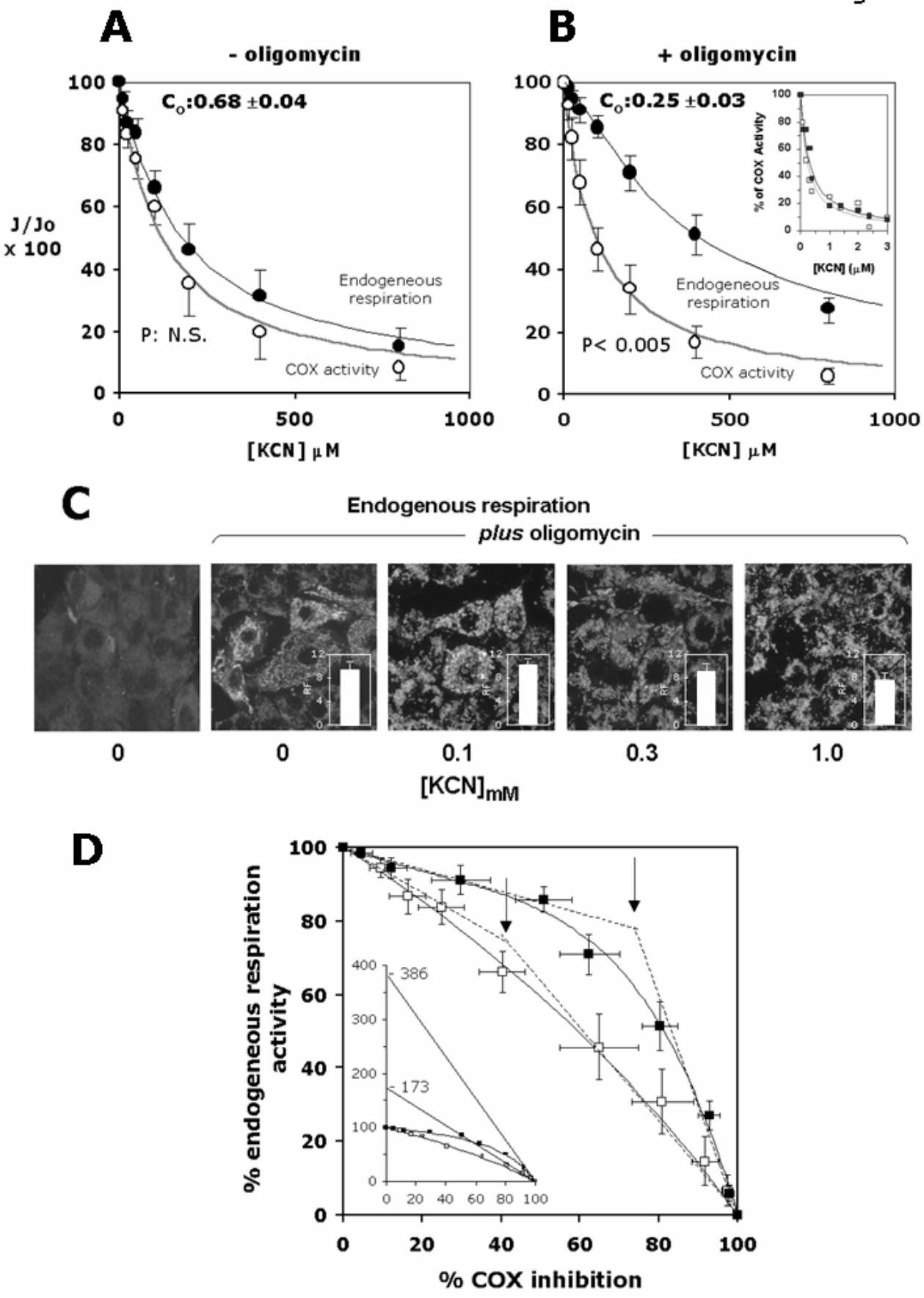

Biochemical Journal Immediate Publication. Published on 13 Mar 2006 as manuscript BJ20060077

Fig. 4

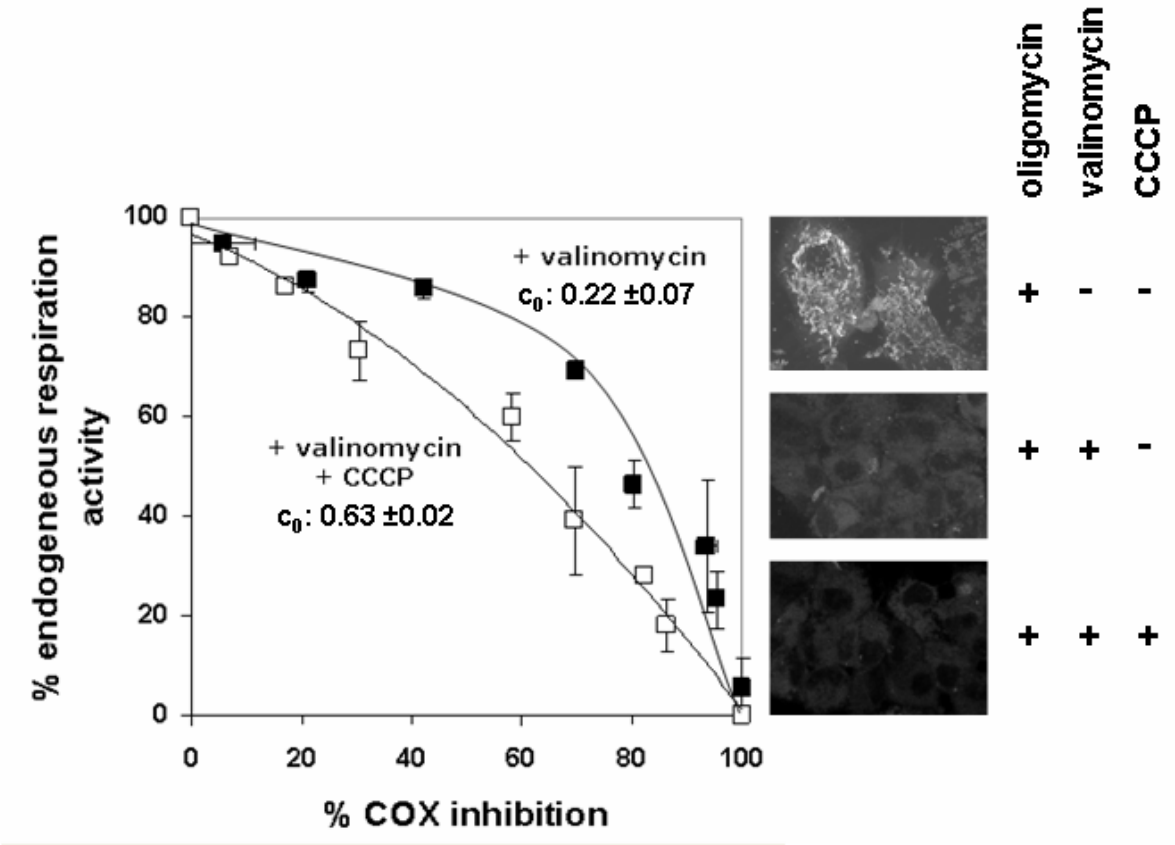

Biochemical Journal Immediate Publication. Published on 13 Mar 2006 as manuscript BJ20060077

Fig. 5

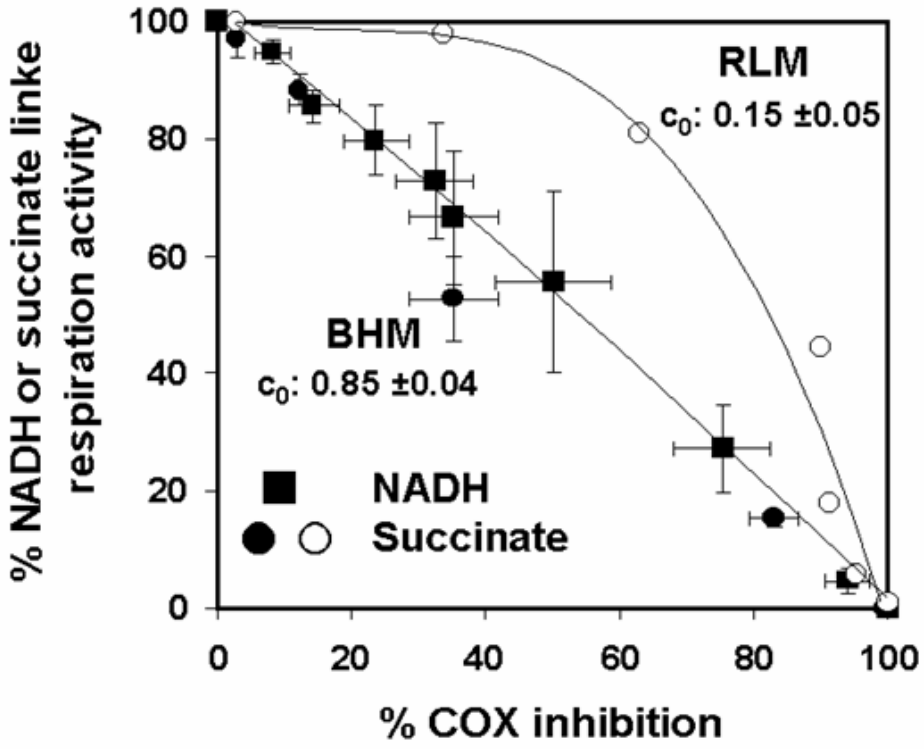

Biochemical Journal Immediate Publication. Published on 13 Mar 2006 as manuscript BJ20060077

Fig. 6

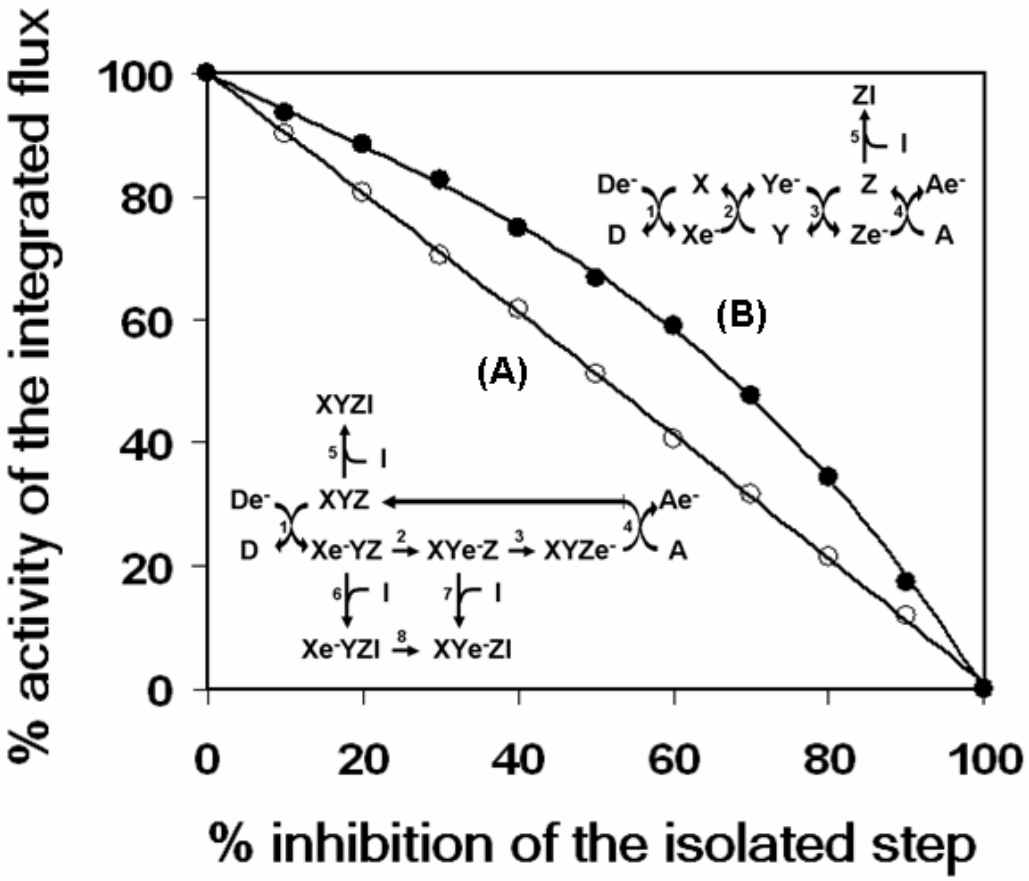

Biochemical Journal Immediate Publication. Published on 13 Mar 2006 as manuscript BJ20060077

Fig. 7

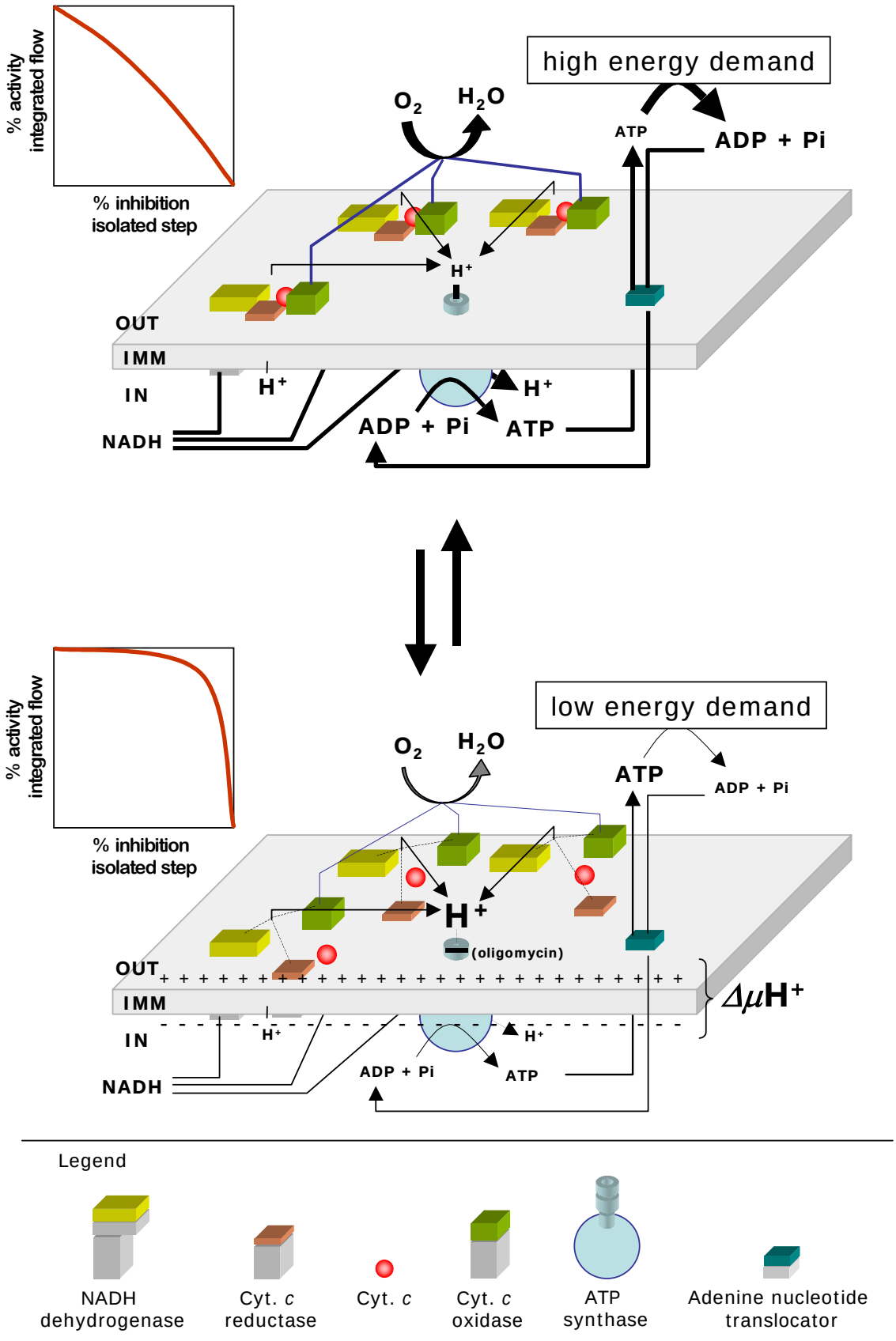

Biochemical Journal Immediate Publication. Published on 13 Mar 2006 as manuscript BJ20060077